Smart Structures and Systems, *Vol. 29*, *No. 1* (*2022*) *41-51*
https://doi.org/10.12989/sss.2022.29.1.041

Unsupervised one-class classification for condition assessment of bridge cables using Bayesian factor analysis

Xiaoyou Wang [a], Lingfang Li[*], Wei Tian [b], Yao Du [c], Rongrong Hou [d] and Yong Xia [e]

Department of Civil and Environmental Engineering, *The Hong Kong Polytechnic University*, *Kowloon*, *Hong Kong*, *PRC*

(*Received April 2*, *2021*, *Revised June 16*, *2021*, *Accepted* July 28, 2021)

Abstract. Cables are critical components of cable-stayed bridges. A structural health monitoring system provides real-time cable tension recording for cable health monitoring. However, the measurement data involve multiple sources of variability, i.e., varying environmental and operational factors, which increase the complexity of cable condition monitoring. In this study, a one-class classification method is developed for cable condition assessment using Bayesian factor analysis (FA). The single-peaked vehicle-induced cable tension is assumed to be relevant to vehicle positions and weights. The Bayesian FA is adopted to establish the correlation model between cable tensions and vehicles. Vehicle weights are assumed to be latent variables and the influences of different transverse positions are quantified by coefficient parameters. The Bayesian theorem is employed to estimate the parameters and variables automatically, and the damage index is defined on the basis of the well-trained model. The proposed method is applied to one cable-stayed bridge for cable damage detection. Significant deviations of the damage indices of Cable SJS11 were observed, indicating a damaged condition in 2011. This study develops a novel method to evaluate the health condition of individual cable using the FA in the Bayesian framework. Only vehicle-induced cable tensions are used and there is no need to monitor the vehicles. The entire process, including the data pre-processing, model training and damage index calculation of one cable, takes only 35 s, which is highly efficient.

Keywords: Bayesian factor analysis; cable condition assessment; damage index; one-class classification; vehicle-induced cable tension

1. Introduction

Long-span stayed-cable bridges usually operate under complex loading and environmental conditions, which may lead to deterioration and vulnerability of bridge components (Li and Ou 2016). As a critical component of cable-stayed bridges, cables were reported to be related to several bridge accidents (Brownjohn *et al*. 2011, Li and Ou 2016, Li *et al*. 2018). In this connection, it is of high necessity to monitor the health conditions of cables to issue early warnings of damage. In recent decades, structural health monitoring (SHM) system has been designed and applied to several long-span stayed-cable bridges worldwide (Ko and Ni 2005, Li and Ou 2016). Accelerometers, strain gauges and fibre optic sensors have been installed on or embedded in cables to record their acceleration and strain responses. However, SHM systems generate large amounts of measurement data. Bridges also usually operate under complicated environmental and operational conditions (e.g., temperature, rain, wind and traffic loads), which vary significantly and may lead to changes in dynamic cable responses (Ko and Ni 2005, Xu and Xia 2011, Farrar and Worden 2012, Li and Ou 2016, Jing *et al*. 2017). It is challenging to process the huge amounts of data efficiently and assess the health condition of cables accurately.

The era of big data has witnessed extensive studies focusing on data mining, aiming at efficient feature extraction and pattern recognition from big data. Statistical pattern recognition implemented by machine learning techniques has been developed into a mature discipline (Farrar and Worden 2012). Given that engineering problems always involve different degrees of uncertainties, statistical pattern recognition approaches stand out as appropriate methods for SHM (Farrar and Worden 2012, Huang *et al*. 2019, Sun *et al*. 2020). The novelty detection, also known as outlier detection, belongs to the unsupervised one-class pattern recognition in which normal data are abundant while abnormal data are unavailable or rare (Markou and Singh 2003a). Data-based SHM has the background of novelty detection. Specifically, researchers can collect sufficient normal data in the initial structural service stage before damage occurs. In addition, the one-class pattern recognition does not need the direct measurement of the sources of variability. Therefore, the unsupervised one-class classification models for novelty detection can be applied to SHM for real-time damage detection, especially when environmental and operational factors are not measured and only dynamic responses are available.

A variety of one-class classification techniques has been

*Corresponding author, Ph.D.,
E-mail: lingfang.li@connect.polyu.hk
[a] Ph.D. Candidate, E-mail: xiaoyou.wang@connect.polyu.hk
[b] Ph.D. Candidate, E-mail: cewei.tian@connect.polyu.hk
[c] Ph.D. Student, E-mail: duyao.du@connect.polyu.hk
[d] Ph.D., E-mail: rongrong.hou@connect.polyu.hk
[e] Professor, E-mail: y.xia@polyu.edu.hk

ISSN: 1738-1584 (Print), 1738-1991 (Online)

developed for novelty detection (Schölkopf *et al*. 1999, Markou and Singh 2003a, b, Hoffmann 2007, Pimentel *et al*. 2014). The basic idea behind these methods is to establish statistical models to explain the variations of training data, and then examine the consistency of the new monitoring data with the model. Observations generated by a novel pattern will lead to obvious deviations distinguishable from the normal data. One-class classification models have also been used for structural damage detection. Representative techniques include principal component analysis (Yan *et al*. 2005a, Sen *et al*. 2019) and its nonlinear interpretations. Examples are kernel principal component analysis and auto-associative neural network (Sohn *et al*. 2001, Yan *et al*. 2005b, Li *et al*. 2010, Reynders *et al*. 2014), factor analysis (FA) (Wang *et al*. 2021), singular value decomposition (Ni *et al*. 2005) and Mahalanobis squared distance (Figueiredo *et al*. 2011). Most studies have used acceleration responses or modal properties for condition assessment of a structure, whilst rare studies on cable condition assessment. Fan *et al*. (2020) proposed a cointegration approach. They extracted a warning index from a cointegrated residual series for cable anomaly warning. The warning threshold needs to be updated annually. Li *et al*. (2018) used the mean of the Gaussian mixture model as the damage index for the condition assessment of a cable pair. However, the method does not apply to the health condition of a single cable.

In the present study, a one-class classification method for cable condition assessment is developed using cable tension data. The Bayesian FA is adopted to establish the relationship between vehicle-induced cable tensions and vehicle information. The variables and parameters in the FA model are estimated using the Bayesian framework. The damage index is defined on the reconstruction error of the FA model. The proposed method is applied to one cable-stayed bridge for cable damage detection.

2. Background

The method developed in this study uses vehicle-induced cable tensions for analysis. Different from the acceleration time history, in which the data oscillate randomly around zero (equilibrium condition), the typical cable tension data are composed of a relatively stable and large value induced by static loads or environmental factors and spikes with small amplitudes, as shown in Fig. 1(a). The spikes are mainly induced by running vehicles. The static load and environmental factor-induced cable tensions are around 2530 kN, and the vehicle-induced tensions are smaller than 130 kN within the one-hour data in Fig. 1(a). The shapes of these spikes, whether single-peak shaped as marked by the red star or multi-peaked as marked by the red circles in Fig. 1(b), are related to the traffic conditions (Li *et al*. 2018). The cable tension will increase monotonically as a single vehicle approaches the cable anchorage. Then, it will drop monotonically as the vehicle moves away. The traffic condition wherein multiple vehicles on different lanes simultaneously passing the cable anchorage position may also result in a similar cable tension shape. However, when multiple vehicles continuously pass by a cable anchorage, the induced spikes may have many small peaks in practice, making the model complex. The cable tension with single peaks, whose effect is simplified as a concentrated force, is the focus of this study. The vehicle-bridge interaction is neglected (Guo and Xu 2001). The single-peak shaped cable tensions are therefore only related to the static loads, the environmental factors, the vehicle weights and the transverse positions (lanes) of the vehicles considering that the longitudinal position is fixed. Accordingly, the model of a single cable tension peak is established as

$$\begin{aligned} T &= T_{\mathrm{V}} + T_{\mathrm{S}} + T_{\mathrm{E}} = \mathbf{CV} + T_{\mathrm{S}} + T_{\mathrm{E}} \\ &= \begin{bmatrix} c_1 & c_2 & \cdots & c_M \end{bmatrix} \begin{bmatrix} v_1 \\ v_2 \\ \vdots \\ v_M \end{bmatrix} + T_{\mathrm{S}} + T_{\mathrm{E}} \end{aligned} \tag{1}$$

$$T_{\mathrm{V}} = \mathbf{CV} = \begin{bmatrix} c_1 & c_2 & \cdots & c_M \end{bmatrix} \begin{bmatrix} v_1 \\ v_2 \\ \vdots \\ v_M \end{bmatrix} \tag{2}$$

where T is the total cable tension peak, and T_{V} is the vehicle-induced cable tension peak. T_{S} is the cable tension induced by the static loads, and T_{E} is the cable tension induced by environmental factors, such as temperature. T_{E}

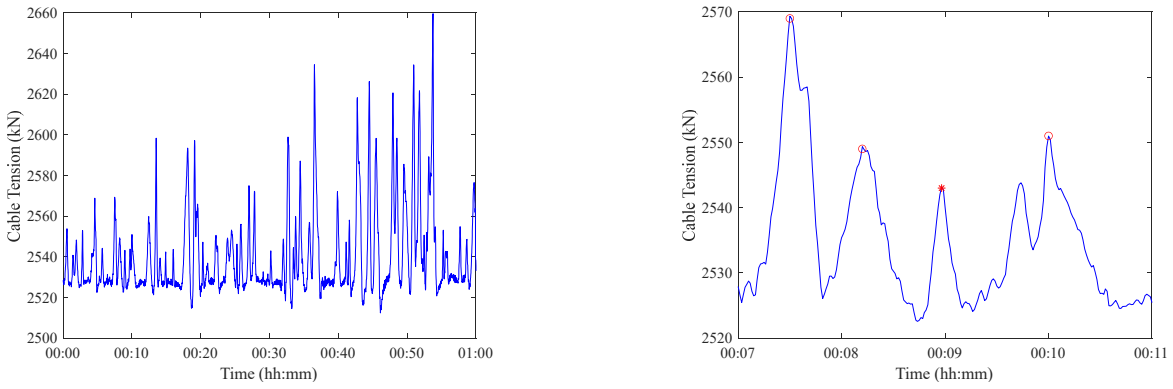

(a) One-hour cable tensions (b) Four-minute cable tensions

Fig. 1 Time history of typical cable tension

is assumed stable in relatively short time duration (as of the cable tension sampling period). $\mathbf{V} = [v_1 \quad v_2 \quad \cdots \quad v_M]^{\mathrm{T}}$ is the equivalent concentrated forces of vehicle weights on different lanes in the same longitudinal position. $\mathbf{C} = [c_1 \quad c_2 \quad \cdots \quad c_M]$ is the corresponding coefficients. M is the number of lanes theoretically. However, for some cables, the effects of some adjacent lanes may be similar, making M smaller than the number of lanes. $\mathbf{V}$ is sparse for most T_{V} because multiple vehicles maintaining the same longitudinal position is not common.

When the tension peaks of a pair of cables on the upstream and downstream sides in the same longitudinal position are available, considering that $\mathbf{V}$ is the same for the cable pair, the model can be written as

$$\begin{bmatrix} T_{\mathrm{u}} \\ T_{\mathrm{d}} \end{bmatrix} = \begin{bmatrix} T_{\mathrm{uV}} \\ T_{\mathrm{dV}} \end{bmatrix} + \begin{bmatrix} T_{\mathrm{uS}} \\ T_{\mathrm{dS}} \end{bmatrix} + \begin{bmatrix} T_{\mathrm{uE}} \\ T_{\mathrm{dE}} \end{bmatrix} = \begin{bmatrix} \mathbf{C}_{\mathrm{u}} \\ \mathbf{C}_{\mathrm{d}} \end{bmatrix} \begin{bmatrix} v_1 \\ v_2 \\ \vdots \\ v_M \end{bmatrix} + \begin{bmatrix} T_{\mathrm{uS}} \\ T_{\mathrm{dS}} \end{bmatrix} + \begin{bmatrix} T_{\mathrm{uE}} \\ T_{\mathrm{dE}} \end{bmatrix} = \begin{bmatrix} c_{\mathrm{u}1} & c_{\mathrm{u}2} & \cdots & c_{\mathrm{u}M} \\ c_{\mathrm{d}1} & c_{\mathrm{d}2} & \cdots & c_{\mathrm{d}M} \end{bmatrix} \begin{bmatrix} v_1 \\ v_2 \\ \vdots \\ v_M \end{bmatrix} + \begin{bmatrix} T_{\mathrm{uS}} \\ T_{\mathrm{dS}} \end{bmatrix} + \begin{bmatrix} T_{\mathrm{uE}} \\ T_{\mathrm{dE}} \end{bmatrix} \tag{3}$$

$$\begin{bmatrix} T_{\mathrm{uV}} \\ T_{\mathrm{dV}} \end{bmatrix} = \begin{bmatrix} \mathbf{C}_{\mathrm{u}} \\ \mathbf{C}_{\mathrm{d}} \end{bmatrix} \begin{bmatrix} v_1 \\ v_2 \\ \vdots \\ v_M \end{bmatrix} = \begin{bmatrix} c_{\mathrm{u}1} & c_{\mathrm{u}2} & \cdots & c_{\mathrm{u}M} \\ c_{\mathrm{d}1} & c_{\mathrm{d}2} & \cdots & c_{\mathrm{d}M} \end{bmatrix} \begin{bmatrix} v_1 \\ v_2 \\ \vdots \\ v_M \end{bmatrix} \tag{4}$$

where subscripts "u" and "d" in the variables and parameters indicate whether they correspond to the upstream or downstream cable.

For a fixed cable (pair), $\mathbf{C}$ ($[\mathbf{C}_{\mathrm{u}} \quad \mathbf{C}_{\mathrm{d}}]^{\mathrm{T}}$) is constant while T_{V} ($[T_{\mathrm{uV}} \quad T_{\mathrm{dV}}]^{\mathrm{T}}$) varies with $\mathbf{V}$. This relation can be estimated by the FA model, which describes the variations of T_{V} ($[T_{\mathrm{uV}} \quad T_{\mathrm{dV}}]^{\mathrm{T}}$) in terms of parameter $\mathbf{C}$ ($[\mathbf{C}_{\mathrm{u}} \quad \mathbf{C}_{\mathrm{d}}]^{\mathrm{T}}$) and the latent variable $\mathbf{V}$. Thus, FA in the sparse Bayesian framework is employed in this study.

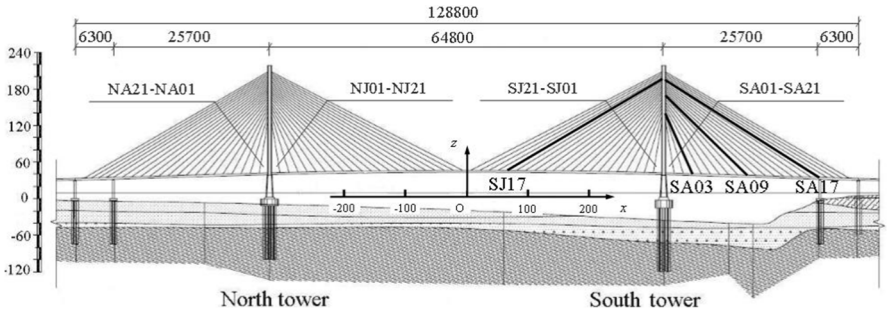

Fig. 2 Configuration of cable-stayed bridge and cable numbering (unit: mm)

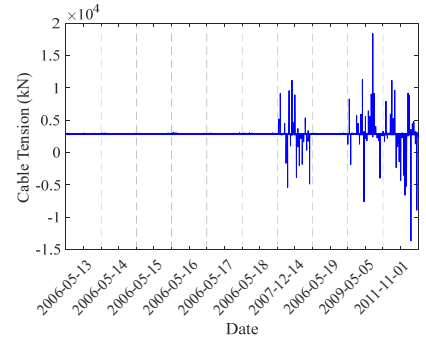

(a) SJS13 cable tensions in ten days

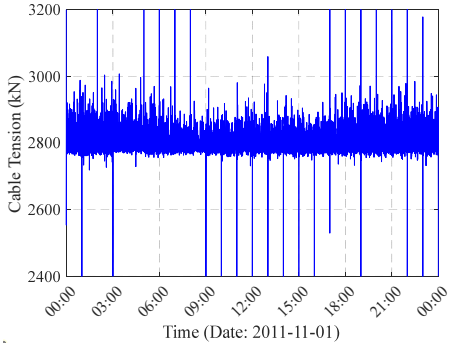

(b) SJS13 cable tensions on 2011-11-01

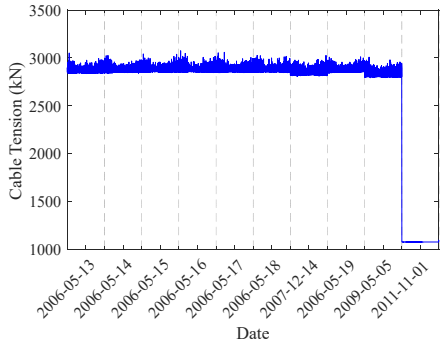

(c) SJX13 cable tensions in ten days

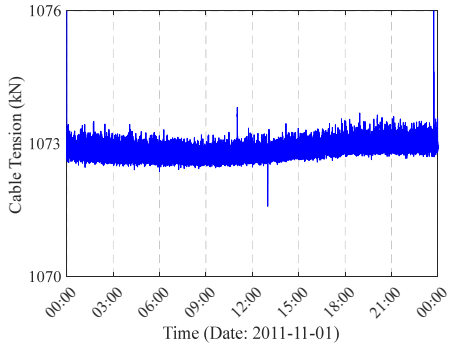

(d) SJX13 cable tensions on 2011-11-01

Fig. 3 Raw SJS13 and SJX13 cable tensions

The desired T_V ($[T_{uV} \quad T_{dV}]^T$) should be first extracted from the raw data before they are fed to the FA. Take an in-service double-tower and double-cable-plane cable-stayed bridge in China as an example, as shown in Fig. 2. Cable pairs are numbered from 01 to 21 on the tower side to the riverside/bank side. The first letter in the tag number 'S/N' represents the south and north sides, respectively. The second letter, 'A/J', represents cables on the bank side and riverside, respectively. In each pair, 'S/X' represents cables on the upstream and downstream sides. For example, SJS08 represents the cable on the upstream side of the eighth cable pair. An SHM system is implemented on this bridge, and all cables are incorporated with anchorage load cells. Cable tensions are monitored with a sampling frequency of 2 Hz.

The raw cable tension data contain outliers and suffer from fault sensor. The tensions of Cables SJS13 and SJX13 are illustrated in Fig. 3. Outliers similar to those in Figs. 3(a) and (b) are removed first as the values are not acceptable, and the remaining data are still feasible for extracting the cable tension peaks. The cable tensions showed in Fig. 3(d) cannot be used. The data remain almost constant within the entire day and are much smaller than those collected earlier, as shown in Fig. 3(c).

The cable tensions are similar to those shown in Fig. 1 after removing the abnormal data. To ensure that the tensions extracted are induced by vehicles, static load-induced cable tension T_S ($[T_{uS} \quad T_{dS}]^T$) and environmental factor-induced cable tension T_E ($[T_{uE} \quad T_{dE}]^T$) should be removed. To this end, two procedures were carried out. In the first step, a "detrend" function in MATLAB is employed to remove the environmental influences and static loads roughly. In the second step, both the peak and start point of a single-peaked shape are identified, and then we calculated their difference as the vehicle-induced tension. Specifically, the peaks are identified by the 'findpeak' function in MATLAB. Accordingly, the vehicle-induced cable tensions (in single-peak or multi-peak shapes) are obtained, as shown in Fig. 4(a). Then, the desired peaks are extracted in accordance with a few criteria. For example, both sides of the peak should decrease monotonically to below zero to ensure the single-peaked shape. The value of the peak should be larger than 10 kN, and the width of the peak should be no less than 10 s. These criteria should be followed to ensure that vehicles, rather than the noise or outlier, induced the extracted peaks. Finally, the extracted T_V are marked and numbered in Fig. 4(b).

The vehicle-induced cable tension peaks of seven cable pairs are extracted. The numbers of extracted single peaks

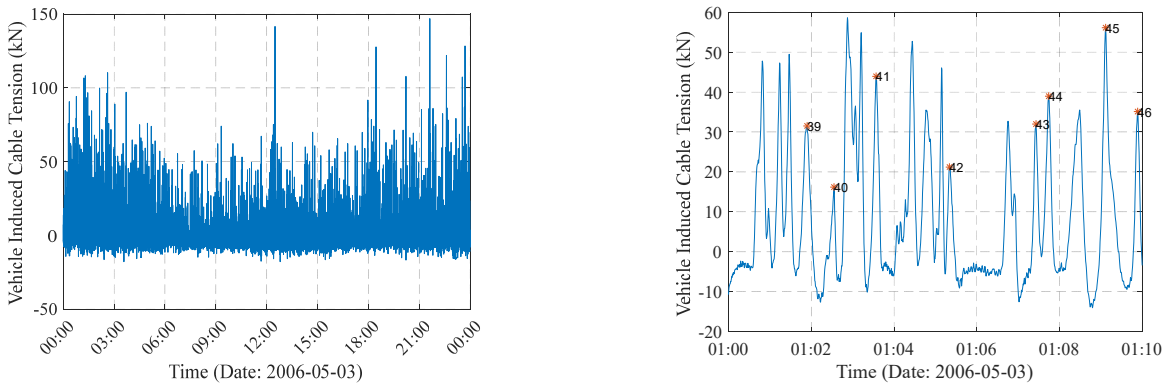

(a) Vehicle-induced cable tensions (b) Extracted T_V

Fig. 4 Extracted vehicle-induced cable tension peaks

Table 1 Numbers of extracted single-peaked cable tension in ten days

Day	Cable pairs						
	SJS/X08	SJS/X09	SJS/X10	SJS/X11	SJS/X12	SJS/X13	SJS/X14
1	834/849 (304)	854/887 (308)	895/426 (200)	844/804 (305)	917/804 (322)	738/741 (276)	671/714 (241)
2	786/858 (292)	820/904 (314)	892/429 (210)	839/816 (307)	900/815 (317)	756/763 (278)	669/721 (253)
3	841/831 (302)	867/907 (310)	932/437 (203)	874/807 (323)	915/775 (330)	758/713 (261)	657/677 (244)
4	903/879 (332)	936/911 (346)	951/430 (203)	870/784 (295)	945/827 (310)	809/798 (296)	747/751 (273)
5	870/865 (303)	916/906 (305)	936/428 (200)	849/778 (293)	913/738 (269)	739/706 (244)	648/675 (225)
6	877/813 (272)	893/879 (324)	900/394 (177)	835/765 (271)	884/745 (276)	740/717 (262)	691/309 (121)
7	760/795 (273)	845/854 (311)	869/392 (175)	810/767 (299)	843/747 (305)	702/678 (253)	602/642 (216)
8	1022/1025 (454)	1042/1054 (448)	1044/713 (330)	946/949 (410)	973/939 (412)	1045/889 (37)	801/834 (334)
9	1069/1056 (408)	1108/1085 (412)	1112/630 (267)	1031/961 (367)	1052/970 (364)	1007/859 (41)	825/803 (255)
10	1285/0 (0)	1285/1179 (455)	1282/797 (309)	1034/1095 (374)	1157/1061 (392)	1181/0 (0)	972/934 (331)

*Note: The values in parentheses indicate the number of extracted peaks for the cable pairs

in ten days are listed in Table 1. No peak satisfying the criteria is extracted of Cables SJX08 and SJX13 on 2011-11-01.

For each cable (cable pair), the extracted peaks form a matrix $\mathbf{F} \in \mathbb{R}^{D\times N}$, where N is the total number of desired extracted peaks. $D = 1$ or 2, when the cable tensions are analysed individually or in pairs, respectively. Subsequently, the matrix $\mathbf{F}$ is fed to the Bayesian FA, which is introduced in the following section.

3. Bayesian FA

The cable tension peaks are extracted as $\mathbf{F} = [\mathbf{F}_1, \mathbf{F}_2, \dots, \mathbf{F}_N] \in \mathbb{R}^{D\times N}$. The equivalent forces are assumed to be unobserved factors denoted by $\mathbf{x}_n$. Their relationship is expressed by the FA model (Bartholomew *et al*. 2011) as

$$\mathbf{F}_n = \mathbf{C}\mathbf{x}_n + \boldsymbol{\varepsilon}_n \ (n = 1, 2, \dots, N) \tag{5}$$

where $\mathbf{F}_n$ is the nth data with the mean $\boldsymbol{\mu} = \sum_{i=1}^{N} \mathbf{F}_i$ subtracted. $\mathbf{C}$ is a $D \times M$ factor loading matrix, whose elements in the ith column (i = 1, …, M) represents the coefficients of vehicle loads on the ith lane. $\boldsymbol{\varepsilon}_n$ is the residual noise vector that follows a Gaussian distribution with a zero-mean and covariance matrix $\boldsymbol{\Psi}$ (Bishop 2006). Specifically, $p(\boldsymbol{\varepsilon}_n) = \mathcal{N}(\boldsymbol{\varepsilon}_n|\mathbf{0}, \boldsymbol{\Psi})$, where $\boldsymbol{\Psi}$ is a $D\times D$ positive semidefinite matrix. In Eq. (5), only $\mathbf{F}_n$ is available whereas latent variables $\mathbf{x}_n$ and parameters $\mathbf{C}$, $\boldsymbol{\Psi}$ and M are all unknown and need to be estimated.

The health condition of cables can also be assessed individually even they are analysed in pairs, namely, $\mathbf{F}_n = [\mathbf{F}_{n\mathrm{u}} \quad \mathbf{F}_{n\mathrm{d}}]^{\mathrm{T}}$.

3.1 Probabilistic framework

Estimating parameters $\mathbf{C}$ and $\boldsymbol{\Psi}$ and variables $\mathbf{x}_n$ from the extracted cable tension peak $\mathbf{F}_n$ is an inverse problem, which can be solved using the Bayes' theorem. The components of the overall Bayesian equation are described as follows.

3.1.1 Prior function

As mentioned previously, M is related to the dimension of $\mathbf{C}$ and needs to be determined. In recent decades, sparse Bayesian learning and the automatic relevance determination (ARD) model have been extensively used to explore a sparse solution (Tipping 2001). Similar to the Bayesian PCA (Bishop 1999), the ARD prior is adopted here in $\mathbf{C}$ for automatic dimension selection. A Gaussian prior is defined over each column of $\mathbf{C}$ as follows

$$p(\mathbf{C}|\boldsymbol{\alpha}) = \prod_{i=1}^{M} \left(\frac{\alpha_i}{2\pi}\right)^{\frac{D}{2}} exp\left\{-\frac{1}{2}\alpha_i \mathbf{c}_i{}^{\mathrm{T}}\mathbf{c}_i\right\} \tag{6}$$

where $\mathbf{c}_i$ is the ith column of $\mathbf{C}$, and α_i is the hyperparameter that governs the precision of the factor loading $\mathbf{c}_i$. An independence among columns $\mathbf{c}_i$ is assumed. In theory, M is no more than the number of lanes and thus initially assumed equal to the number of lanes. If the actual dimensionality is less than the assumed value, some α_i will approach infinity and enforce the corresponding columns in $\mathbf{C}$ to zero. For simplicity, non-informative priors of $\boldsymbol{\Psi}$ is defined.

The prior $p(\mathbf{x})$ is assumed to follow $\mathcal{N}(\mathbf{x}|\mathbf{0}, \mathbf{I})$, that is

$$p(\mathbf{x}) = \prod_{n=1}^{N} p(\mathbf{x}_n) = \left(\frac{1}{2\pi}\right)^{\frac{MN}{2}} \prod_{n=1}^{N} exp\left\{-\frac{\mathbf{x}_n{}^{\mathrm{T}}\mathbf{x}_n}{2}\right\} \tag{7}$$

The prior independence of $\mathbf{x}$, $\mathbf{C}$ and $\boldsymbol{\Psi}$ is assumed here as $p(\mathbf{x}, \mathbf{C}, \boldsymbol{\Psi}) = p(\mathbf{x})p(\mathbf{C})p(\boldsymbol{\Psi})$.

3.1.2 Likelihood function

The likelihood function of the cable tension conditional on $\mathbf{x}$, $\mathbf{C}$ and $\boldsymbol{\Psi}$ is $p(\mathbf{F}|\mathbf{C}, \boldsymbol{\Psi}, \mathbf{x})$, which follows the Gaussian distribution $\mathcal{N}(\mathbf{F}|\mathbf{C}\mathbf{x}, \boldsymbol{\Psi})$ (Bishop 2006) as

$$p(\mathbf{F}|\mathbf{C}, \boldsymbol{\Psi}, \mathbf{x}) = \prod_{n=1}^{N} p(\mathbf{F}_n|\mathbf{C}, \boldsymbol{\Psi}, \mathbf{x}_n) = \left(\frac{1}{2\pi}\right)^{\frac{DN}{2}} |\boldsymbol{\Psi}|^{-\frac{N}{2}} \prod_{n=1}^{N} exp\left\{-\frac{1}{2}(\mathbf{F}_n - \mathbf{C}\mathbf{x}_n)^{\mathrm{T}}\boldsymbol{\Psi}^{-1}(\mathbf{F}_n - \mathbf{C}\mathbf{x}_n)\right\} \tag{8}$$

3.1.3 Posterior function

On the basis of the Bayesian theorem, the posterior probability density function (PDF) of the latent variable $\mathbf{x}_n$ conditional on parameters $\mathbf{C}$ and $\boldsymbol{\Psi}$ is

$$\begin{aligned} p(\mathbf{x}|\mathbf{F}, \mathbf{C}, \boldsymbol{\Psi}) &= c_0^{-1} p(\mathbf{F}|\mathbf{C}, \boldsymbol{\Psi}, \mathbf{x})p(\mathbf{x}) = c_0^{-1} p(\mathbf{F}, \mathbf{x}|\mathbf{C}, \boldsymbol{\Psi}) \propto \prod_{n=1}^{N} exp\left\{-\frac{1}{2}(\mathbf{F}_n - \mathbf{C}\mathbf{x}_n)^{\mathrm{T}}\boldsymbol{\Psi}^{-1}(\mathbf{F}_n - \mathbf{C}\mathbf{x}_n) - \frac{\mathbf{x}_n{}^{\mathrm{T}}\mathbf{x}_n}{2}\right\} \\ &\propto \prod_{n=1}^{N} exp\left\{\mathbf{x}_n{}^{\mathrm{T}}\mathbf{C}^{\mathrm{T}}\boldsymbol{\Psi}^{-1}\mathbf{F}_n - \frac{1}{2}\mathbf{x}_n{}^{\mathrm{T}}(\mathbf{I} + \mathbf{C}^{\mathrm{T}}\boldsymbol{\Psi}^{-1}\mathbf{C})\mathbf{x}_n\right\} \end{aligned} \tag{9}$$

It is noted that Eq. (9) is quadratic with respect to $\mathbf{x}_n$, and thus the posterior PDF of $\mathbf{x}_n$ follows the Gaussian distribution. By comparing Eq. (9) with the PDF of a Gaussian distribution, the mean and second moment of the posterior $\mathbf{x}_n$ are obtained (Bishop 2006) as

$$\mathbb{E}_{\mathbf{x}_n}[\mathbf{x}_n|\mathbf{F}_n, \mathbf{C}, \boldsymbol{\Psi}] = \boldsymbol{\Sigma}_{\mathbf{x}_n}\mathbf{C}^{\mathrm{T}}\boldsymbol{\Psi}^{-1}\mathbf{F}_n \tag{10}$$

$$\begin{aligned} &\mathbb{E}_{\mathbf{x}_n}[\mathbf{x}_n\mathbf{x}_n{}^{\mathrm{T}}|\mathbf{F}_n, \mathbf{C}, \boldsymbol{\Psi}] \\ &= \boldsymbol{\Sigma}_{\mathbf{x}_n} + \mathbb{E}_{\mathbf{x}_n}[\mathbf{x}_n|\mathbf{F}_n, \mathbf{C}, \boldsymbol{\Psi}] \times \mathbb{E}_{\mathbf{x}_n}[\mathbf{x}_n|\mathbf{F}_n, \mathbf{C}, \boldsymbol{\Psi}]^{\mathrm{T}} \end{aligned} \tag{11}$$

where $\boldsymbol{\Sigma}_{\mathbf{x}_n} = (\mathbf{I} + \mathbf{C}^{\mathrm{T}}\boldsymbol{\Psi}^{-1}\mathbf{C})^{-1}$ is the covariance matrix of $\mathbf{x}_n$. The posterior PDF of the parameters is

$$p(\mathbf{C},\boldsymbol{\Psi}|\mathbf{F},\mathbf{x},\boldsymbol{\alpha}) = c_1^{-1}p(\mathbf{F}|\mathbf{C},\boldsymbol{\Psi},\mathbf{x})p(\mathbf{x})p(\mathbf{C}|\boldsymbol{\alpha})p(\boldsymbol{\Psi}) \propto |\boldsymbol{\Psi}|^{-\frac{N}{2}}\prod_{n=1}^{N} exp\left\{-\frac{1}{2}(\mathbf{F}_n-\mathbf{C}\mathbf{x}_n)^{\mathrm{T}}\boldsymbol{\Psi}^{-1}(\mathbf{F}_n-\mathbf{C}\mathbf{x}_n)-\frac{\mathbf{x}_n{}^{\mathrm{T}}\mathbf{x}_n}{2}\right\}\times\prod_{i=1}^{M} exp\left\{-\frac{1}{2}\alpha_i\mathbf{c}_i{}^{\mathrm{T}}\mathbf{c}_i\right\} \tag{12}$$

However, the statistics of $\mathbf{C}$ and $\boldsymbol{\Psi}$ cannot be directly obtained from Eq. (12). The reason is the intractable integral in the evidence. This is a general problem when the Bayesian theorem is applied to high-dimensional or nonlinear problems. Asymptotic or numerical sampling techniques can be applied to obtain the approximate or numerical solutions, including the Laplace approximation, variation inference, expectation-maximisation (EM) algorithm and Markov Chain Monte Carlo sampling techniques (Beck and Katafygiotis 1998, Bishop 1999, 2006, Tipping 2001, Wang *et al*. 2020). The EM technique is applicable to Bayesian models with latent variables whose posterior statistics can be obtained. In this study, the posterior mean and second moment of the latent variable are computed according to Eqs. (10) and (11). Consequently, the efficient EM technique is employed and will be introduced in the next section.

3.2 EM algorithm

The EM technique consists of two iterative steps: the E step and M step (Bishop 2006). In the E step, the expectation of the complete-data likelihood function concerning the variable $\mathbf{x}$ is calculated. In the subsequent M step, the expectation is maximised with respect to the parameters, from which the maximum a posterior (MAP) of the parameters can be solved. The detailed procedures are as follows.

In the E step, the expectation is calculated as

$$\mathbb{E}_{\mathbf{x}}[\ln p(\mathbf{F},\mathbf{x}|\mathbf{C},\boldsymbol{\Psi})+\ln p(\mathbf{C}|\boldsymbol{\alpha})] = -\frac{(M+D)N}{2}\ln(2\pi)-\frac{N}{2}\ln|\boldsymbol{\Psi}|+\frac{D}{2}\sum_{n=1}^{M} ln\left(\frac{\alpha_i}{2\pi}\right)-\sum_{n=1}^{M}\left(\frac{1}{2}\alpha_i\mathbf{c}_i{}^{\mathrm{T}}\mathbf{c}_i\right) -\sum_{n=1}^{N}\left[\frac{1}{2}\mathbf{F}_n{}^{\mathrm{T}}\boldsymbol{\Psi}^{-1}\mathbf{F}_n\right]-\sum_{n=1}^{N}\frac{1}{2}\mathbb{E}_{\mathbf{x}_n}(\mathbf{x}_n{}^{\mathrm{T}}\mathbf{x}_n)+\sum_{n=1}^{N}\left[\mathbf{F}_n{}^{\mathrm{T}}\boldsymbol{\Psi}^{-1}\mathbf{C}\mathbb{E}_{\mathbf{x}_n}[\mathbf{x}_n]-\frac{1}{2}\mathbb{E}_{\mathbf{x}_n}(\mathbf{x}_n{}^{\mathrm{T}}\mathbf{C}^{\mathrm{T}}\boldsymbol{\Psi}^{-1}\mathbf{C}\mathbf{x}_n)\right] \tag{13}$$

where the logarithm form is used for the convenience of calculation.

In the M step, Eq. (13) is maximised concerning each parameter as

$$\frac{\partial}{\partial\mathbf{C}}\{\mathbb{E}_{\mathbf{x}}[\ln p(\mathbf{F},\mathbf{x}|\mathbf{C},\boldsymbol{\Psi})]+\ln p(\mathbf{C}|\boldsymbol{\alpha})\} = \sum_{n=1}^{N}\boldsymbol{\Psi}^{-1}\mathbf{F}_n\mathbb{E}_{\mathbf{x}_n}[\mathbf{x}_n]^{\mathrm{T}}-\sum_{n=1}^{N}\boldsymbol{\Psi}^{-1}\mathbf{C}\mathbb{E}_{\mathbf{x}_n}[\mathbf{x}_n\mathbf{x}_n{}^{\mathrm{T}}]-\mathbf{C}\mathrm{diag}(\alpha_i)=0 \tag{14}$$

$$\frac{\partial}{\partial\boldsymbol{\Psi}^{-1}}\{\mathbb{E}_{\mathbf{x}}[\ln p(\mathbf{F},\mathbf{x}|\mathbf{C},\boldsymbol{\Psi})]+\ln p(\mathbf{C}|\boldsymbol{\alpha})\} = \frac{1}{2}\sum_{n=1}^{N}\left[\boldsymbol{\Psi}-\mathbf{F}_n\mathbf{F}_n{}^{\mathrm{T}}\right]+\sum_{n=1}^{N}\mathbf{F}_n\mathbb{E}_{\mathbf{x}_n}[\mathbf{x}_n]^{\mathrm{T}}\mathbf{C}^{\mathrm{T}}-\frac{1}{2}\sum_{n=1}^{N}\mathbf{C}\mathbb{E}_{\mathbf{x}_n}[\mathbf{x}_n\mathbf{x}_n{}^{\mathrm{T}}]\mathbf{C}^{\mathrm{T}}=0 \tag{15}$$

Thus, one has

$$\boldsymbol{\Psi}^{-1}\mathbf{C}+\mathbf{C}\mathrm{diag}(\alpha_i)\left(\sum_{n=1}^{N}\mathbb{E}_{\mathbf{x}_n}[\mathbf{x}_n\mathbf{x}_n{}^{\mathrm{T}}]\right)^{-1} = \boldsymbol{\Psi}^{-1}\left(\sum_{n=1}^{N}\mathbf{F}_n\mathbb{E}_{\mathbf{x}_n}[\mathbf{x}_n]^{\mathrm{T}}\right)\left(\sum_{n=1}^{N}\mathbb{E}_{\mathbf{x}_n}[\mathbf{x}_n\mathbf{x}_n{}^{\mathrm{T}}]\right)^{-1} \tag{16}$$

$$\boldsymbol{\Psi} = \frac{1}{N}\sum_{n=1}^{N}\left(\mathbf{F}_n\mathbf{F}_n{}^{\mathrm{T}}-2\mathbf{F}_n\mathbb{E}_{\mathbf{x}_n}[\mathbf{x}_n]^{\mathrm{T}}\mathbf{C}^{\mathrm{T}}+\mathbf{C}\mathbb{E}_{\mathbf{x}_n}[\mathbf{x}_n\mathbf{x}_n{}^{\mathrm{T}}]\mathbf{C}^{\mathrm{T}}\right) \tag{17}$$

$\mathbf{C}$ is solved from Eq. (16) using the Sylvester function, and $\boldsymbol{\Psi}$ is calculated from Eq. (17). Accordingly, the MAP estimate of $\boldsymbol{\alpha}$ is obtained by

$$\hat{\boldsymbol{\alpha}} = \underset{\boldsymbol{\alpha}}{argmax}\, p(\boldsymbol{\alpha}|\mathbf{F},\boldsymbol{\Psi}) = \underset{\boldsymbol{\alpha}}{argmax}\, p(\mathbf{F}|\boldsymbol{\Psi},\boldsymbol{\alpha}) = \underset{\boldsymbol{\alpha}}{argmax}\int p(\mathbf{F}|\mathbf{C},\boldsymbol{\Psi})p(\mathbf{C}|\boldsymbol{\alpha})d\mathbf{C} \tag{18}$$

The Laplace approximation is used to get the asymptotic solution of this integral (Bishop 1999). Then, $\hat{\alpha}_i$ is estimated as

$$\hat{\alpha}_i = \frac{D}{\mathbf{c}_i{}^{\mathrm{T}}\mathbf{c}_i}, \qquad i=1,2,\dots,M \tag{19}$$

The coupled E and M steps proceed by initialising parameters $\mathbf{C}$ and $\boldsymbol{\Psi}$, evaluating the statistics of the latent variable $\mathbf{x}_n$ and calculating $\hat{\alpha}_i$. The process is repeated until the convergence criterion is satisfied. Note that the EM algorithm may suffer from the problem of local optimum, depending on the probability distribution. Therefore, it is suggested to try multiple times of EM algorithm under different initializations and then select the best solution, that is, the maximum probability when substituting the solutions into the posterior PDF.

3.3 Damage index

As the latent variables $\mathbf{x}_n$ follows the Gaussian distribution, the MAP estimate is equal to the mean in Eq. (5), that is, $\mathbf{x}_n^{\mathrm{MAP}} = \mathbb{E}_{\mathbf{x}_n}[\mathbf{x}_n|\mathbf{F}_n,\mathbf{C},\boldsymbol{\Psi}]$. The estimated $\mathbf{C}$ and $\boldsymbol{\Psi}$ are substituted into Eq. (5) to calculate the reconstruction

error as

$$\boldsymbol{e}_n = \mathbf{F}_n - \mathbf{C}\mathbf{x}_n^{\mathrm{MAP}} \tag{20}$$

If cables are assessed in pairs ($D = 2$) in Eq. (5), the reconstruction error in Eq. (20) is a vector $\boldsymbol{e}_n = [e_{n\mathrm{u}} \quad e_{n\mathrm{d}}]^{\mathrm{T}}$. $e_{n\mathrm{u}}$ and $e_{n\mathrm{d}}$ represent the reconstruction error corresponding to upstream and downstream cables, respectively. A normalised damage index is defined as

$$DI_n = \sqrt{\left(\frac{e_{n\mathrm{u}}}{\mathbf{F}_{n\mathrm{u}}}\right)^2 + \left(\frac{e_{n\mathrm{d}}}{\mathbf{F}_{n\mathrm{d}}}\right)^2} \tag{21}$$

The damage index in Eq. (21) is scaled by dividing the corresponding tension value instead of directly using the Euclidean norm of the reconstruction error $\boldsymbol{e}_n$ in the traditional methods (Yan *et al*. 2005a, Sen *et al*. 2019, Wang *et al*. 2021) on structural damage detection under varying temperatures. Such a treatment is based on the fact that the training data in this study are collected over limited days. They may not contain the variations in vehicle weights of the test data. Accordingly, using the normalised damage index may avoid false-positive when unseen vehicles occur. After a pair of cables are judged to be damaged according to Eq. (21), the damage index of individual cable can be computed as

$$DI_{n\mathrm{u}} = \left|\frac{e_{n\mathrm{u}}}{\mathbf{F}_{n\mathrm{u}}}\right| \tag{22}$$

$$DI_{n\mathrm{d}} = \left|\frac{e_{n\mathrm{d}}}{\mathbf{F}_{n\mathrm{d}}}\right| \tag{23}$$

Therefore, when the data of cable pairs are available, it is recommended to assess the condition of the cables in pair preliminarily ($D = 2$ in Eq. (5)), which can save time in model training. The condition of each cable can be evaluated individually after the cable pair is initially judged as damaged. If the data are not provided in pair, then the damage condition of each cable is assessed individually ($D = 1$ in Eq. (5)). $\boldsymbol{e}_n$ will be scalar, and the damage index is directly calculated as $DI_n = |e_n/\mathbf{F}_n|$.

4. Summary of the proposed method

The proposed method has the following steps:

1. Eliminate the static and slow-varying component of the cable tensions for each cable (or cable pair). Extract the value of desired peak $\mathbf{F}_n$. Set the training data and test data.
2. Set M equal to the number of traffic lanes first and initialise $\mathbf{C}^{(0)}$ and $\boldsymbol{\Psi}^{(0)}$. Calculate the mean of the training data $\boldsymbol{\mu} = \frac{1}{N}\sum_{n=1}^{N}\mathbf{F}_n$. Update the training data $\mathbf{F}_n$ with the mean $\boldsymbol{\mu}$ removed.
3. Calculate unknown variables and parameters with the training data. In the jth iteration,
4. Given $\mathbf{C}^{(j-1)}$ and $\boldsymbol{\Psi}^{(j-1)}$:
5. Update $\mathbb{E}_{\mathbf{x}_n}[\mathbf{x}_n|\mathbf{F}_n,\mathbf{C},\boldsymbol{\Psi}]^{(j)}$ and $\mathbb{E}_{\mathbf{x}_n}[\mathbf{x}_n\mathbf{x}_n{}^{\mathrm{T}}|\mathbf{F}_n,\mathbf{C},\boldsymbol{\Psi}]^{(j)}$ using Eqs. (10) and (11);
6. Update $\boldsymbol{\alpha}^{(j)}$ using Eq. (19);
7. Update $\mathbf{C}^{(j)}$ and $\boldsymbol{\Psi}^{(j)}$ using Eqs. (16) and (17), respectively.
8. Let $j = j + 1$. Then, repeat Steps 3 to 7 until the convergence criterion is satisfied, namely, $\left\|\boldsymbol{\Psi}^{(j)} - \boldsymbol{\Psi}^{(j-1)}\right\|/\left\|\boldsymbol{\Psi}^{(j)}\right\| \le Tol$ (e.g., $Tol = 1 \times 10^{-4}$).
9. On the basis of the determined $\mathbf{C}$ and $\boldsymbol{\Psi}$, calculate $\hat{\mathbf{x}}_n$ of the training dataset $\mathbf{F}_n$ (including the training data and test data) using Eq. (12) for individual cable (or cable pair). Then, re-generate a new dataset $\mathbf{F}_n{}' = \mathbf{C}\hat{\mathbf{x}}_n$ according to Eq. (5). Note that the entire dataset $\mathbf{F}_n$ should be subtracted by the mean $\boldsymbol{\mu}$ of the training data.
10. Calculate the damage index according to Eq. (21). Evaluate the health condition of each cable (or cable pair) following the damage index in Eqs. (22) and (23).

5. A case study

In this study, the measured cable tensions of seven cable pairs (SJS08 to SJS14 and SJX08 to SJX14) in the bridge described previously in ten days (2006-05-12 to 2006-05-19, 2007-12-14, 2009-05-05 and 2011-11-01) are used for analysis. One of the 14 cables was damaged in 2011. The purpose of this study is to detect the damaged cable using the available cable tension data. Accordingly, the datasets collected during the first nine days (the cables were in a healthy state) are used for model training. The estimated model is applied to damage detection on the last day.

As mentioned previously, the processed cable tensions can be analysed in pairs, which will save time for model training. Therefore, Cables SJS/X09, SJS/X10, SJS/X11, SJS/X12 and SJS/X14 are analysed in pairs, that is, $D = 2$ in Eq. (5). Cables SJS08 and SJS13 have to be assessed individually ($D = 1$) because the data of their downstream cables are abnormal. The cable tensions extracted in the first nine days are set as the training data and that of the tenth day as the test data. When cable tensions are analysed in pairs, the two cables on the upstream and downstream sides reach the peak simultaneously to ensure that the peak is induced by the same vehicle condition. In other words, the number of datasets should be the values in parentheses in Table 1. The training data and test data of SJS/X09 are plotted as an example in Fig. 6.

Subsequently, the proposed FA analysis is applied to the training data. $\mathbf{C}^{(0)}$ is initialised randomly following the uniform distribution in the interval of (0, 1). $M = 6$ as the bridge has six lanes (three in each direction). $\boldsymbol{\Psi}^{(0)}$ is initialised to be diagonal to ensure the property of positive semi-definite. A small $\boldsymbol{\Psi}^{(0)}$ will slow down the convergence speed. By contrast, a large $\boldsymbol{\Psi}^{(0)}$ may enforce the corresponding column in $\mathbf{C}$ to be zero. Therefore, $\boldsymbol{\Psi}$ is initialised as a 2×2 matrix with diagonal elements of 0.5 for all cable pairs or 0.5 for the individual cable. The convergence criterion of the iteration process is set as $\left\|\boldsymbol{\Psi}^{(j)} - \boldsymbol{\Psi}^{(j-1)}\right\|/\left\|\boldsymbol{\Psi}^{(j)}\right\| \le 1\times10^{-4}$. The model is trained following the procedures summarized in Section 4. Given the space limitation, only the iteration process for the cable

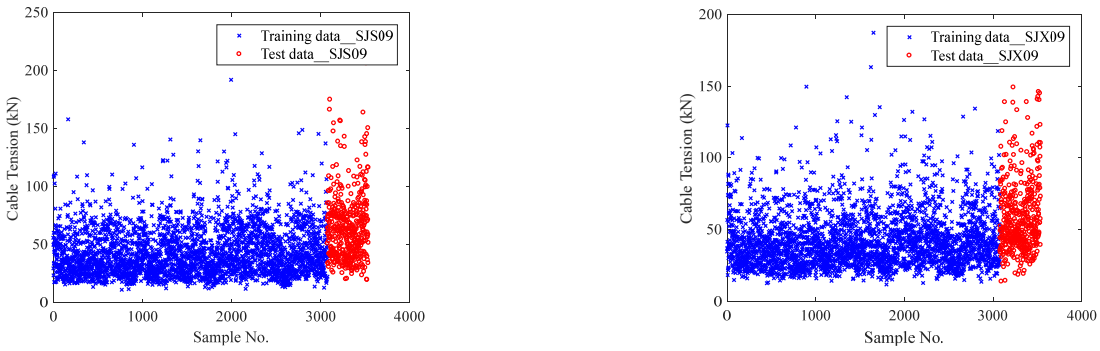

SJS09 SJX09

Fig. 6 Training data and test data of the cable pair SJS/X09

Table 2 Iterative identification process for the variable and parameters of the cable pair SJS/X11

Iteration No.	$\boldsymbol{\alpha}$	$\mathbf{C}$	$\mathbf{x}_1$	M	$\boldsymbol{\Psi}$
0		$\begin{bmatrix}0.92 & 0.35 & 0.60 & 0.47 & 0.16 & 0.46\\ 0.16 & 0.08 & 0.38 & 0.99 & 0.94 & 0.94\end{bmatrix}$		6	$\begin{bmatrix}0.5 & 0\\ 0 & 0.5\end{bmatrix}$
100	$\begin{Bmatrix}0.01\\0.08\\0.03\\0.02\\0.03\\0.02\end{Bmatrix}$	$\begin{bmatrix}13.36 & 4.97 & 8.22 & 5.55 & 1.07 & 5.47\\ 0.22 & 0.29 & 2.83 & 8.75 & 8.80 & 8.33\end{bmatrix}$	$\begin{Bmatrix}2.70\\1.01\\1.72\\1.31\\0.40\\1.28\end{Bmatrix}$	6	$\begin{bmatrix}7.43 & -0.74\\ -0.74 & 4.80\end{bmatrix}$
200	$\begin{Bmatrix}0.01\\0.07\\0.02\\0.01\\0.02\\0.01\end{Bmatrix}$	$\begin{bmatrix}14.79 & 5.43 & 9.42 & 7.29 & 2.34 & 7.15\\ 1.42 & 0.75 & 3.88 & 10.25 & 9.89 & 9.78\end{bmatrix}$	$\begin{Bmatrix}2.45\\0.90\\1.50\\0.99\\0.17\\0.98\end{Bmatrix}$	6	$\begin{bmatrix}8.13 & -0.18\\ -0.18 & 5.29\end{bmatrix}$
282	$\begin{Bmatrix}0.01\\0.07\\0.02\\0.01\\0.02\\0.01\end{Bmatrix}$	$\begin{bmatrix}15.02 & 5.43 & 9.60 & 7.55 & 2.53 & 7.40\\ 1.58 & 0.82 & 4.03 & 10.47 & 10.05 & 9.99\end{bmatrix}$	$\begin{Bmatrix}1.17\\0.41\\0.63\\0.21\\-0.18\\0.22\end{Bmatrix}$	6	$\begin{bmatrix}8.27 & -0.10\\ -0.10 & 5.37\end{bmatrix}$

*Note: The number of training data in the cable pair SJS/X11 is 2875. Only the first component, x_1, is listed here as an example due to the space limitation

pair SJS/X11 is listed in Table 2. The EM process takes 282 iterations to converge. As the process proceeds, no component of $\boldsymbol{\alpha}$ approaches infinity. One phenomenon is that the identified $\mathbf{C}$ and $\mathbf{x}_n$ are full, not as expected. The reason is that D is less than M in the study, making the model with the ARD prior do not ensure a unique MAP solution of $\mathbf{C}$, and therefore cannot uniquely identify the latent factor $\mathbf{x}_n$, either. To ensure a unique solution, surplus degrees of freedom should be removed and more restrictions on parameters are needed (Murphy 2012). Nevertheless, it's demonstrated that the non-identifiability does not affect the predictive performance of the FA model (Murphy 2012). The method provides interpretable solutions of the parameters and variables and performs well for anomaly detection, since the target of this study is to use the FA model to check the consistency of the training data and test data, but not for vehicles identification.

The damage index is calculated using the determined $\mathbf{C}$ and $\boldsymbol{\Psi}$ and according to Eq. (21). The damage indices of five cable pairs (i.e., SJS/X09, SJS/X10, SJS/X11, SJS/X12 and SJS/X14) and Cables SJS08 and SJS13 are plotted in Fig. 7. The cable pair XJS/X11 shows significant deviations of the damage indices on 2011-11-01, while the other cables maintain similar damage indices as those of the former days. This finding indicates that one of the cable pair SJS/X11 is damaged. Accordingly, the individual damage index of SJS11 and SJX11 is calculated according to Eqs. (22) and (23) and plotted in Fig. 8. The comparison results show that the damage index of SJX11 remains comparable within 10 days, whereas that of SJS11 exhibits significant growth in the test data. Therefore, Cable SJS11 can be concluded as the damaged one on 2011-11-01.

All calculations are carried out on a PC with the specifications of i7-8700 CPU and 20 GB RAM. Although the proposed method needs many iterations to converge, the calculation of each iteration takes less than 1 s. The entire process, including the peak extraction, model training and damage index calculation of the cable pair SJS/X11, takes only 35 s. The condition assessment of all cables takes only approximately 5 min. Overall, the proposed method has the

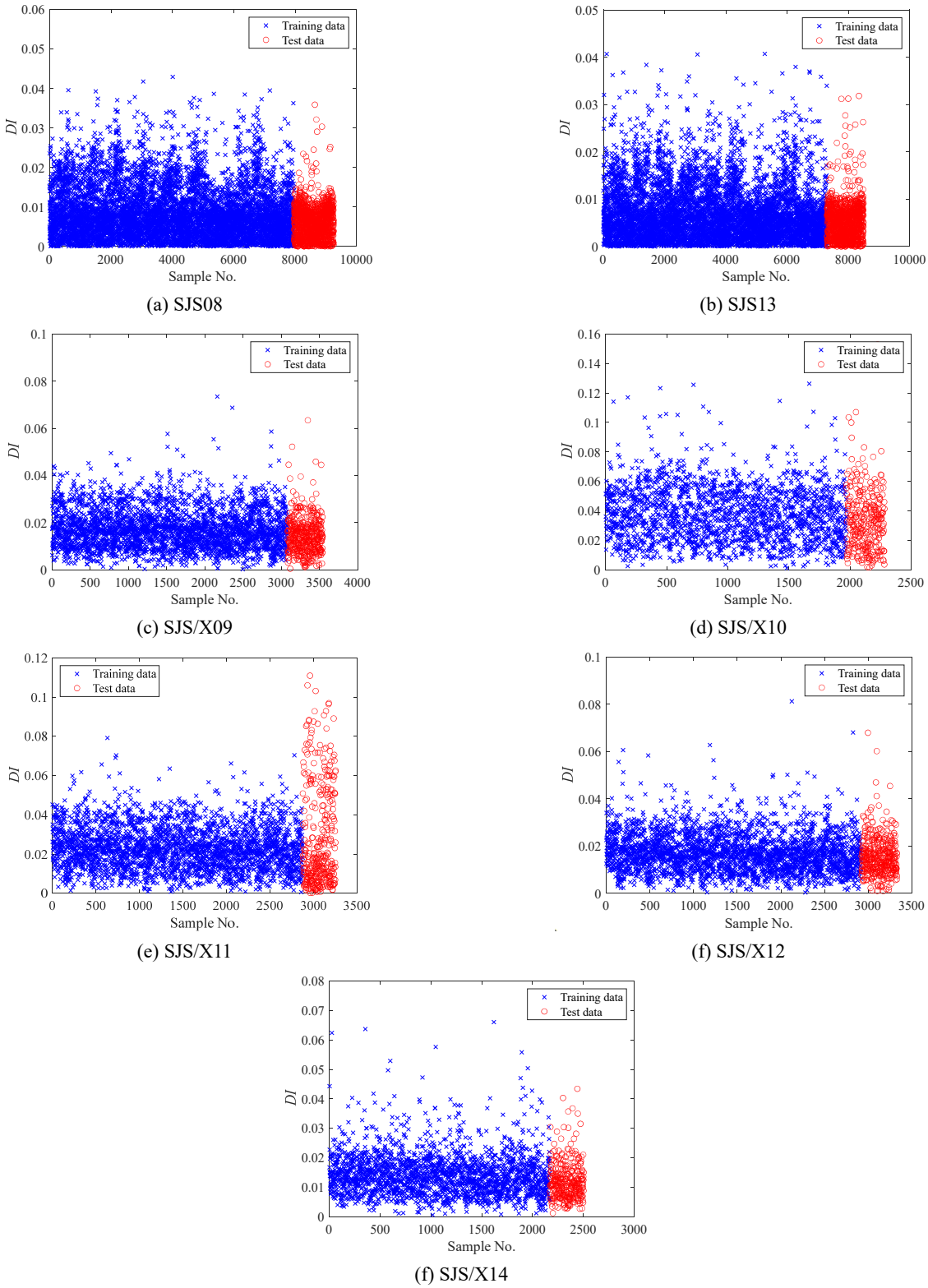

(a) SJS08

(b) SJS13

(c) SJS/X09

(d) SJS/X10

(e) SJS/X11

(f) SJS/X12

(f) SJS/X14

Fig. 7 Damage indices of all cables

advantage of high efficiency.

6. Conclusions

A one-class classification method for cable condition assessment is developed in this study using the Bayesian FA. The traffic-induced cable tensions with the single-peaked shape are extracted as the dataset for analysis. The FA is adopted to establish the model between the cable tensions and vehicles. All unknown parameters and variables in the FA model are estimated automatically in the Bayesian probabilistic frameworks. The reconstruction error of the model is defined as the damage index for the cable

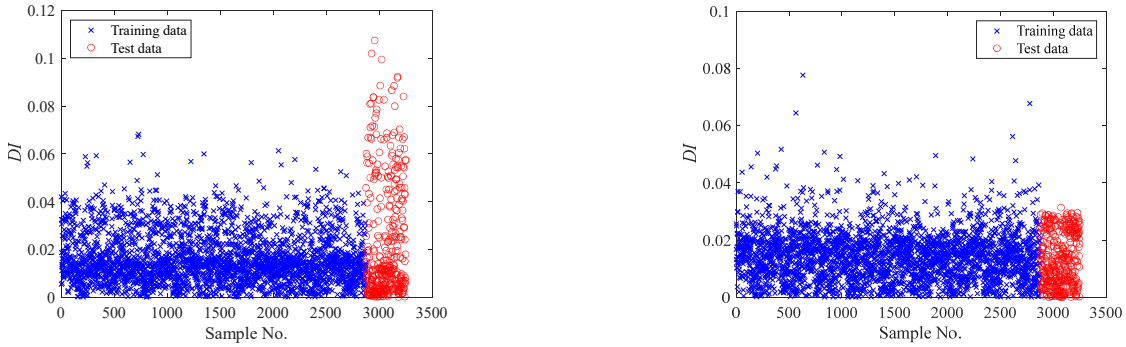

(a) SJS11 (b) SJX11

Fig. 8 Damage indices of Cables SJS11 and SJX11

anomaly detection. The method is applied to a cable-stayed bridge. The results indicate that Cable SJS11 was damaged in 2011. The proposed method is demonstrated to be efficient and effective.

Acknowledgments

The authors are grateful to the organisers of the 1st International Project Competition for SHM (IPC-SHM, 2020) for generously providing the excellent opportunities during the COVID-19 and invaluable data from the actual structures. Our gratitude goes to Professor Hui Li and Professor Billie F. Spencer Jr., Chairs of IPC-SHM, 2020. This research is also supported by the Key-Area Research and Development Program of Guangdong Province (Project No. 2019B111106001) and Research Grants Council of HKSAR−General Research Fund (Project No. 15201920).

References

Bartholomew, D.J., Knott, M. and Moustaki, I. (2011), *Latent Variable Models and Factor Analysis*: *A Unified Approach*, John Wiley & Sons.

Beck, J.L. and Katafygiotis, L.S. (1998), "Updating models and their uncertainties. I: Bayesian statistical framework", *J. Eng. Mech.*, **124**(4), 455-461. https://doi.org/10.1061/(ASCE)0733-9399(1998)124:4(455)

Bishop, C.M. (1999), "Bayesian PCA", Advances in Neural Information Processing Systems, pp. 382-388.

Bishop, C.M. (2006), *Pattern Recognition and Machine Learning*, New York, Springer.

Brownjohn, J.M., Stefano, A.D., Xu, Y.-L., Wenzel, H. and Aktan, A.E. (2011), "Vibration-based monitoring of civil infrastructure: challenges and successes", *J. Civil Struct. Health Monitor.*, **1**, 79-95. https://doi.org/10.1007/s13349-011-0009-5

Fan, Z.Y., Huang, Q., Ren, Y., Zhu, Z.Y. and Xu, X. (2020), "A cointegration approach for cable anomaly warning based on structural health monitoring data: An application to cable-stayed bridges", *Adv. Struct. Eng.*, **23**(13), 2789-2802. https://doi.org/10.1177/1369433220924793

Farrar, C.R. and Worden, K. (2012), *Structural Health Monitoring*: *A Machine Learning Perspective*, John Wiley & Sons.

Figueiredo, E., Park, G., Farrar, C.R., Worden, K. and Figueiras, J. (2011), "Machine learning algorithms for damage detection under operational and environmental variability", *Struct. Health Monitor.*, **10**(6), 559-572. https://doi.org/10.1177/1475921710388971

Guo, W.H. and Xu, Y.L. (2001), "Fully computerized approach to study cable-stayed bridge-vehicle interaction", *J. Sound Vib.*, **248**(4), 745-761. https://doi.org/10.1006/jsvi.2001.3828

Hoffmann, H. (2007), "Kernel PCA for novelty detection", *Pattern Recogn.*, **40**(3), 863-874. https://doi.org/10.1016/j.patcog.2006.07.009

Huang, Y., Shao, C., Wu, B., Beck, J.L. and Li, H. (2019), "State-of-the-art review on Bayesian inference in structural system identification and damage assessment", *Adv. Struct. Eng.*, **22**(6), 1329-1351. https://doi.org/10.1177/1369433218811540

Jing, H., Xia, Y., Li, H., Xu, Y. and Li, Y. (2017), "Excitation mechanism of rain–wind induced cable vibration in a wind tunnel", *J. Fluids Struct.*, **68**, 32-47.

Ko, J. and Ni, Y.Q. (2005), "Technology developments in structural health monitoring of large-scale bridges", *Eng. Struct.*, **27**(12), 1715-1725. https://doi.org/10.1016/j.engstruct.2005.02.021

Li, H. and Ou, J. (2016), "The state of the art in structural health monitoring of cable-stayed bridges", *J. Civil Struct. Health Monitor.*, **6**(1), 43-67. https://doi.org/10.1007/s13349-015-0115-x

Li, H., Li, S., Ou, J. and Li, H. (2010), "Modal identification of bridges under varying environmental conditions: temperature and wind effects", *Struct. Control Health Monitor.*, **17**(5), 495-512. https://doi.org/10.1002/stc.319

Li, S., Wei, S., Bao, Y. and Li, H. (2018), "Condition assessment of cables by pattern recognition of vehicle-induced cable tension ratio", *Eng. Struct.*, **155**, 1-15. https://doi.org/10.1016/j.engstruct.2017.09.063

Markou, M. and Singh, S. (2003a), "Novelty detection: a review-Part 1: Statistical approaches", *Signal Process.*, **83**(12), 2481-2497. https://doi.org/10.1016/j.sigpro.2003.07.018

Markou, M. and Singh, S. (2003b), "Novelty detection: a review-Part 2: Neural network based approaches", *Signal Process.*, **83**(12), 2499-2521. https://doi.org/10.1016/j.sigpro.2003.07.019

Murphy, K.P. (2012), *Machine Learning*: *A Probabilistic Perspective*, Cambridge: MIT Press, Cambridge, UK.

Ni, Y.Q., Hua, X.G., Fan, K.Q. and Ko, J.M. (2005), "Correlating modal properties with temperature using long-term monitoring data and support vector machine technique", *Eng. Struct.*, **27**(12), 1762-1773. https://doi.org/10.1016/j.engstruct.2005.02.020

Pimentel, M.A., Clifton, D.A., Clifton, L. and Tarassenko, L. (2014), "A review of novelty detection", *Signal Process.*, **99**, 215-249. https://doi.org/10.1016/j.sigpro.2013.12.026

Reynders, E., Wursten, G. and De Roeck, G. (2014), "Output-only structural health monitoring in changing environmental conditions by means of nonlinear system identification", *Struct. Health Monitor.*, **13**(1), 82-93.

https://doi.org/10.1177/1475921713502836

Schölkopf, B., Williamson, R.C., Smola, A.J., Shawe Taylor, J. and Platt, J.C. (1999), Support vector method for novelty detection, NIPS, Citeseer.

Sen, D., Erazo, K., Zhang, W., Nagarajaiah, S. and Sun, L. (2019), "On the effectiveness of principal component analysis for decoupling structural damage and environmental effects in bridge structures", *J. Sound Vib*., **457**, 280-298. https://doi.org/10.1016/j.jsv.2019.06.003

Sohn, H., Worden, K. and Farrar, C.R. (2001), "Novelty detection under changing environmental conditions", Smart Structures and Materials 2001: Smart Systems for Bridges, Structures, and Highways, International Society for Optics and Photonics.

Sun, L., Shang, Z., Xia, Y., Bhowmick, S. and Nagarajaiah, S. (2020), "Review of bridge structural health monitoring aided by big data and artificial intelligence: from condition assessment to damage detection", *J. Struct. Eng*., **146**(5), 04020073. https://doi.org/10.1061/(ASCE)ST.1943-541X.0002535

Tipping, M.E. (2001), "Sparse Bayesian learning and the relevance vector machine", *J. Mach. Learn. Res*., **1**, 211-244. https://doi.org/10.1162/15324430152748236

Wang, X., Hou, R., Xia, Y. and Zhou, X. (2020), "Structural damage detection based on variational Bayesian inference and delayed rejection adaptive Metropolis algorithm", *Struct. Health Monitor*., 1475921720921256. https://doi.org/10.1177/1475921720921256

Wang, X., Li, L., Beck, J.L. and Xia, Y. (2021), "Sparse Bayesian factor analysis for structural damage detection under unknown environmental conditions", *Mech. Syst. Signal Process*., **154**, 107563. https://doi.org/0.1016/j.ymssp.2020.107563

Xu, Y.L. and Xia, Y. (2011). *Structural Health Monitoring of Long-Span Suspension Bridges*, London: CRC Press, London, UK.

Yan, A.M., Kerschen, G., De Boe, P. and Golinval, J.C. (2005a), "Structural damage diagnosis under varying environmental conditions-Part I: A linear analysis", *Mech. Syst. Signal Process*., **19**(4), 847-864. https://doi.org/10.1016/j.ymssp.2004.12.002

Yan, A.M., Kerschen, G., De Boe, P. and Golinval, J.C. (2005b), "Structural damage diagnosis under varying environmental conditions-Part II: Local PCA for non-linear cases", *Mech. Syst. Signal Process*., **19**(4), 865-880. https://doi.org/10.1016/j.ymssp.2004.12.003